STANFORD RESEARCH INSTITUTE
Menlo Park, California 94025 · U.S.A.

September 1972

STEREOPSIS ERROR ANALYSIS

by

David Nitzan

Artificial Intelligence Center

Technical Note 71

SRI Project 1530

The research reported herein was supported at SRI by the Advanced Research Projects Agency of the Department of Defense, monitored by the U.S. Army Research Office-Durham under Contract DAHC04 72 C 0008.

ABSTRACT

The error due to image quantization in stereoscopically evaluated range is analyzed, using a simple camera model and assuming that the image planes of the two cameras are coplanar. The "best" position and the uncertainty space for a point in space are calculated on the basis of the quantized image coordinates of that point in the two cameras.

1. Introduction

In this technical note we develop the mathematical formulas for determination of range values and their extreme errors on the basis of quantized stereoscopic pictures of a scene.

Two cameras, with lenses L_ℓ and L_r, are located at a distance D from each other to determine the components of a distance r from the midpoint between L_ℓ and L_r and an object point B, as shown in Fig. 1. The focal length of each camera is f. The picture plane is of size w x w and is quantized into n x n cells, each of size d. We wish to calculate the error introduced by the digitization process in determining the x, y, and z of r.

Let us denote the coordinates of the image point on the left and right pictures by (x_ℓ, z_ℓ) and (x_r, z_r), respectively. For convenience, we shall use mirrored image planes, instead of the actual ones. To simplify the analysis, let us first assume that $z_\ell = z_r = 0$, i.e., the projecting rays (of lengths r_ℓ and r_r) lie in the plane defined by the parallel optical axes of the two cameras (see Fig. 1). We shall later remove this assumption. Furthermore, we shall also assume that the optical axes are parallel to the y axis; the effects of panning and tilting of the cameras may be added later by using standard transformation rules.

2. Quantization Errors and Uncertainty Regions

The top view of the stereopsis plane, in which both $x_\ell > 0$ and $x_r > 0$, is shown in Fig. 2. Due to the quantization process, we obtain picture coordinates x_ℓ^* and x_r^*, and thus arrive at Point B* whose coordinates are x* and y* instead of the real point, Point B, whose coordinates are x and y. By inspection,

$$\frac{y^*}{x^*+\frac{1}{2}D} = \frac{f}{x_\ell^*}$$

and

$$\frac{y^*}{x^*-\frac{1}{2}D} = \frac{f}{x_r^*}$$

Solving for x* and y*, we get

$$x^* = D \frac{x_\ell^* + x_r^*}{2(x_\ell^* - x_r^*)} \tag{1}$$

and

$$y^* = D \frac{f}{x_\ell^* - x_r^*} \tag{2}$$

For given quantized values of x_ℓ^* and x_r^*, the quantization errors δ_ℓ and δ_r (see Fig. 2) introduce uncertainty into the computed values of $x = x^* - \Delta x$ and $y = y^* - \Delta y$. A quadrilateral uncertainty region is obtained by varying δ_ℓ and δ_r according to $-d/2 < \delta_\ell < d/2$ and $-d/2 < \delta_r < d/2$, as shown in Fig. 3. The extreme x and y values of the quadrilateral uncertainty region determine a rectangle defined by $x_{min} \le x \le x_{max}$ and $y_{min} \le y \le y_{max}$. This rectangle constitutes a worst-case uncertainty region. It is marked in Fig. 3 by a dotted rectangle.

The values of δ_ℓ and δ_r in the above four cases of extreme quantization errors are given in Table I. It can be shown that the values of $-\delta_\ell - \delta_r$ and $-\delta_\ell + \delta_r$ affect the expressions for x, y, Δx, and Δy. The resulting expressions are given in Table I for each of the four cases. Note that in Cases 2 and 3 (see, for example, Fig. 3), $\Delta y = 0$ and the values of Δx are equal in magnitude but opposite in sign.

3. Object Zones

So far we have assumed that $x_\ell^* > 0$ and $x_r^* > 0$, i.e., Point B* is to the right of L_r. There are, however, two more possibilities to consider: $x_\ell^* > 0$ and $x_r^* < 0$, in which Point B* is to the right of L_ℓ and to the left of L_r, and $x_\ell^* < 0$ and $x_r^* < 0$, in which Point B* is to the left of L_ℓ. Note that the fourth possibility, $x_\ell^* < 0$ and $x_r^* > 0$, is forbidden. Note also that by excluding $x_\ell^* = 0$ and/or $x_r^* = 0$, we have tacitly assumed that picture-cell boundaries exist at $x_\ell = 0$ and at $x_r = 0$. Generally,

Table I. Calculated Expressions for x, y, Δx, and Δy in Four Cases of Extreme Quantization Errors

Variable	Case 1	Case 2	Case 3	Case 4
δ_ℓ	$-d/2$	$d/2$	$-d/2$	$d/2$
δ_r	$d/2$	$d/2$	$-d/2$	$-d/2$
$-\delta_\ell-\delta_r$	0	$-d$	d	0
$-\delta_\ell+\delta_r$	d	0	0	$-d$
x	$D\dfrac{x_\ell^*+x_r^*}{2(x_\ell^*-x_r^*+d)}$	$D\dfrac{x_\ell^*+x_r^*-d}{2(x_\ell^*-x_r^*)}$	$D\dfrac{x_\ell^*+x_r^*+d}{2(x_\ell^*-x_r^*)}$	$D\dfrac{x_\ell^*+x_r^*}{2(x_\ell^*-x_r^*-d)}$
y	$D\dfrac{f}{x_\ell^*-x_r^*+d}$	$D\dfrac{f}{x_\ell^*-x_r^*}$	$D\dfrac{f}{x_\ell^*-x_r^*}$	$D\dfrac{f}{x_\ell^*-x_r^*-d}$
Δx	$D\dfrac{d(x_\ell^*+x_r^*)}{2(x_\ell^*-x_r^*)(x_\ell^*-x_r^*+d)}$	$D\dfrac{d}{2(x_\ell^*-x_r^*)}$	$-D\dfrac{d}{2(x_\ell^*-x_r^*)}$	$-D\dfrac{d(x_\ell^*+x_r^*)}{2(x_\ell^*-x_r^*)(x_\ell^*-x_r^*-d)}$
Δy	$D\dfrac{fd}{(x_\ell^*-x_r^*)(x_\ell^*-x_r^*+d)}$	0	0	$-D\dfrac{fd}{(x_\ell^*-x_r^*)(x_\ell^*-x_r^*-d)}$

therefore, there are three possible object zones, as shown in Fig. 4: Zone R ($x_\ell^*>0$ and $x_r^*>0$), Zone M ($x_\ell^*>0$ and $x_r^*<0$), and Zone L ($x_\ell^*<0$ and $x_r^*<0$). Any of these zones is characterized by the algebraic inequality $x_\ell \geq x_r$ (if Point B is at infinity, then $x_\ell = x_r$). Therefore, assuming that the two cameras have identical quantization cells, then $x_\ell^* \geq x_r^*$.

Quadrilateral and worst-case rectangular uncertainty regions in each of the above zones are illustrated in Fig. 4. Each uncertainty region is defined by two uncertainty beams, $-d/2 < \delta_\ell < d/2$ and $-d/2 < \delta_r < d/2$. The quadrilateral (or rectangular) uncertainty region in Zone R is similar to the one in Fig. 3. Its extreme boundaries are $x_{min} = x_1$, $x_{max} = x_4$, $y_{min} = y_1$, and $y_{max} = y_4$, where each subscript denotes the "case" number, as defined in Table I. Keeping the positive x_ℓ^* fixed, we "fan" the right uncertainty beam counterclockwise, thus causing the uncertainty region to move to the left and into Zone M, until some negative x_r^* is reached. Unlike Zone R, the extreme x boundaries of the uncertainty region in Zone M are $x_{min} = x_2$ and $x_{max} = x_3$, whereas the extreme y boundaries remain $y_{min} = y_1$ and $y_{max} = y_4$. Next, we keep the negative x_r^* fixed and fan the left uncertainty beam counterclockwise, again causing the uncertainty region to move to the left until reaching the position in Zone L. The extreme x values have changed again, i.e., $x_{min} = x_4$ and $x_{max} = x_1$, and the extreme y values are again $y_{min} = y_1$ and $y_{max} = y_4$.

4. Quantization Coordinate Numbers

So far we have used the quantization coordinates x_ℓ^* and x_r^* to determine the values of x, y, and their quantization errors. To be more general, we may, alternatively, use the picture indices corresponding to x_ℓ^* and x_r^*. Following the assumption that picture-cell boundaries exist at $x_\ell = 0$ and $x_r = 0$, then

$$\left.\begin{aligned} x_\ell^* &= (n_\ell - \tfrac{1}{2})d \\ x_r^* &= (n_r - \tfrac{1}{2})d \end{aligned}\right\} \quad n_\ell \geq n_r \qquad (3)$$

where n_ℓ and n_r are quantization coordinate numbers, which are nonzero

integers, and the inequality $n_\ell \geq n_r$ follows from the inequality $x_\ell^* \geq x_r^*$.

The quantized image shift is defined as

$$x_\Delta^* \equiv x_\ell^* - x_r^* = (n_\ell - n_r)d \tag{4}$$

Assuming that D, f, and d are constant, we note in Table I that y and Δy in every case and Δx in Cases 2 and 3 are each a function of the image shift only. However, x in every case and Δx in Cases 1 and 4 are each a function of both the image shift and the <u>average</u> quantized x coordinate

$$\bar{x}_p^* \equiv \frac{x_\ell^* + x_r^*}{2} = \frac{(n_\ell + n_r - 1)d}{2} \tag{5}$$

We consider first y and Δy vs. the quantized image shift, $n_\ell - n_r$. Based on the expressions given in Table I, plots of $y_{min} = y_1$ and $y_{max} = y_4$ vs. $n_\ell - n_r$ are shown in Fig. 5. As expected, both y_{min} and y_{max} increase as $n_\ell - n_r$ decreases. Note that $y_{min, n_\ell - n_r} = y_{max, n_\ell - n_r + 2}$. Also note in Fig. 5 that as $n_\ell - n_r$ decreases, the worst-case error $y_{max} - y_{min}$ increases. More information about the error in y may be obtained by separating $y_{max} - y_{min}$ into its components $\Delta y_{min} = \Delta y_1$ and $\Delta y_{max} = -\Delta y_4$. Based on Table I, plots of Δy_{min} and Δy_{max} vs. $n_\ell - n_r$ are shown in Fig. 6.

The errors in x in Zone M are inversely proportional to $n_\ell - n_r$, whereas all other errors (errors in x in Zones R and L and errors in y in all zones) are approximately inversely proportional to $(n_\ell - n_r)^2$. Furthermore, since $n_\ell \geq 1$ and $n_r \leq 1$, then $n_\ell - n_r = |n_\ell| + |n_r|$ and, therefore, the <u>magnitudes</u> of the errors in both x and y in Zone M are smaller than those in Zones R and L for the same x_ℓ^* and x_r^* magnitudes. If $x_\ell^* = -x_r^*$, then $\bar{x}_p^* = 0$, i.e., Point B* is along the axis of symmetry between the two cameras (cf. Figs. 3 and 4). For this special case, the expressions for x and Δx in Cases 2 and 3 (see Table I) are reduced to

$$x_{max} = \Delta x_{max} = -x_{min} = -\Delta x_{min} = \frac{D}{4n_\ell} \tag{6}$$

Referring to Fig. 4, the area of the uncertainty region in Zone M is minimized for a given projecting ray if the two projecting rays are perpendicular. The locus of such minimum regions is a semicircle centered at x = 0 whose diameter is D. Unfortunately, this locus is likely to be too close to the cameras to have any practical value.

5. Vertical Coordinates

So far we have assumed that the object point lies on the x-y plane. We now lift this restriction and let Point B be in a three-dimensional space, as shown in Fig. 7. The ideally parallel optical axes of the two cameras point along the y direction, as before. The left and right projecting rays pierce their corresponding image planes at two points whose picture coordinates are $(x_\ell; z_\ell)$ and $(x_r; z_r)$ respectively. The above analysis for determination of the x and y coordinates assuming z = 0 is valid with no change for the general case in which $z \neq 0$ because x and y depend only on x_ℓ and x_r, not on z_ℓ or z_r.

If there were no difference between the tilt angles of the two cameras, the two projecting rays would meet at Point B (see Fig. 7). In this case, the intersection of the plane defined by the two rays and the vertical plane y = f is a straight line parallel to the x-y plane and at a distance $z_\ell = z_r$ from this plane. By inspection of similar triangles in Fig. 7, $z_\ell/z = z_r/z = f/y$; hence, $z = z_\ell y/f$, and the "best estimate" of z is $z^* = z_\ell^* y^*/f$. Substituting $y^*/f = D/(x_\ell^* - x_r^*)$ from (2), and replacing z_ℓ^* by the average value

$$\bar{z}_p^* = \tfrac{1}{2}(z_\ell^* + z_r^*) \qquad (7)$$

just in case $z_\ell^* \neq z_r^*$ due to error in camera alignment, we find that

$$z^* = D\bar{z}_p^*/x_\Delta^* \qquad (8)$$

Since each of the quantized coordinates x_ℓ^*, x_r^*, z_ℓ^*, and z_r^* may have an error that varies between -d/2 and d/2, the value of z may vary between

z_{min} and z_{max}, where

$$z_{min} = D \frac{\bar{z}_p^* - \frac{1}{2}d}{x_\Delta^* + d} \tag{9}$$

and

$$z_{max} = D \frac{\bar{z}_p^* + \frac{1}{2}d}{x_\Delta^* - d} \tag{10}$$

6. Three-Dimensional Uncertainty Space

The error in estimating x, y, and z due to the picture quantization is confined to a hexahedral uncertainty space formed by the two three-dimensional uncertainty beams as shown in Fig. 8 (note that $x_\ell^* > D/2$ in Fig. 8 by mistake). Each of the uncertainty beams has the shape of a four-sided pyramid. The side views of these beams along the -x axis are shown in Fig. 8(a). These side views overlap because we have decided to approximate the ranges $z_\ell = z_\ell^* \pm \frac{1}{2}d$ and $z_r = z_r^* \pm \frac{1}{2}d$ by the average range $\frac{1}{2}(z_\ell^* + z_r^*) \pm \frac{1}{2}d$. (Note that z_ℓ or z_r is not necessarily within this average range.) On the basis of this approximation, the uncertainty space is hexahedral with four vertical sides, as shown in Fig. 8(b). Without this assumption the two uncertainty beams may not meet and the averaging process will become unnecessarily complex.

Let us summarize the above analysis in terms of the quantization numbers

$$n_{\ell x} = (x_\ell^*/d) + \tfrac{1}{2} \tag{11}$$

$$n_{rx} = (x_r^*/d) + \tfrac{1}{2} \tag{12}$$

$$n_{\ell z} = (z_\ell^*/d) + \tfrac{1}{2} \tag{13}$$

and

$$n_{rz} = (z_r^*/d) + \tfrac{1}{2} \ . \tag{14}$$

Using the abbreviations

$$n_{\Delta} = n_{\ell x} - n_{rx} = x_{\Delta}^*/d \tag{15}$$

$$\bar{n}_x = \tfrac{1}{2}(n_{\ell x} + n_{rx}) = (\bar{x}_p^*/d) + \tfrac{1}{2} \tag{16}$$

and

$$\bar{n}_z = \tfrac{1}{2}(n_{\ell z} + n_{rz}) = (\bar{z}_p^*/d) + \tfrac{1}{2}, \tag{17}$$

(4), (5), and (7) become

$$x_{\Delta}^* = n_{\Delta} d \tag{18}$$

$$\bar{x}_p^* = (\bar{n}_x - \tfrac{1}{2})d \tag{19}$$

and

$$\bar{z}_p^* = (\bar{n}_z - \tfrac{1}{2})d \tag{20}$$

Hence, (1), (2), and (8) are expressed as

$$v^* = \begin{pmatrix} x^* \\ y^* \\ z^* \end{pmatrix} = \begin{pmatrix} D(\bar{n}_x - \tfrac{1}{2})/n_{\Delta} \\ Df/(n_{\Delta} d) \\ D(\bar{n}_z - \tfrac{1}{2})/n_{\Delta} \end{pmatrix} \tag{21}$$

and the expressions in Table I in conjunction with Fig. 4 are reduced to the following:

$$x_{min} = \begin{cases} D(\bar{n}_x - \tfrac{1}{2})/(n_{\Delta}+1) & \text{if } n_{\ell x} > 0 \text{ and } n_{rx} > 0 \text{ (Zone R)} \\ D(\bar{n}_x - 1)/n_{\Delta} & \text{if } n_{\ell x} > 0 \text{ and } n_{rx} < 0 \text{ (Zone M)} \\ D(\bar{n}_x - \tfrac{1}{2})/(n_{\Delta}-1) & \text{if } n_{\ell x} < 0 \text{ and } n_{rx} < 0 \text{ (Zone L)} \end{cases} \tag{22}$$

$$x_{max} = \begin{cases} D(\bar{n}_x - \tfrac{1}{2})/(n_{\Delta}-1) & \text{if } n_{\ell x} > 0 \text{ and } n_{rx} > 0 \text{ (Zone R)} \\ D\bar{n}_x/n_{\Delta} & \text{if } n_{\ell x} > 0 \text{ and } n_{rx} < 0 \text{ (Zone M)} \\ D(\bar{n}_x - \tfrac{1}{2})/(n_{\Delta}+1) & \text{if } n_{\ell x} < 0 \text{ and } n_{rx} < 0 \text{ (Zone L)} \end{cases} \tag{23}$$

$$y_{min} = \frac{Df}{d(n_{\Delta}+1)} \tag{24}$$

$$y_{max} = \frac{Df}{d(n_\Delta - 1)} \tag{25}$$

$$z_{min} = \begin{cases} D(\bar{n}_z - 1)/(n_\Delta + 1) & \text{if } \bar{n}_z > \tfrac{1}{2} \\ D(\bar{n}_z - 1)/(n_\Delta - 1) & \text{if } \bar{n}_z \le \tfrac{1}{2} \end{cases} \tag{26}$$

and

$$z_{max} = \begin{cases} D\bar{n}_z/(n_\Delta - 1) & \text{if } \bar{n}_z \ge \tfrac{1}{2} \\ D\bar{n}_z/(n_\Delta + 1) & \text{if } \bar{n}_z < \tfrac{1}{2} \end{cases} \tag{27}$$

The relative errors in x, y, and z are found from (21) through (27) to be as follows:

$$\left(\frac{\Delta x}{x}\right)_{min} = \frac{x^*}{x_{min}} - 1 = \begin{cases} 1/n_\Delta & \text{if } n_{\ell x} > 0 \text{ and } n_{rx} > 0 \text{ (Zone R)} \\ 1/[2(\bar{n}_x - 1)] & \text{if } n_{\ell x} > 0 \text{ and } n_{rx} < 0 \text{ (Zone M)} \\ -1/n_\Delta & \text{if } n_{\ell x} < 0 \text{ and } n_{rx} < 0 \text{ (Zone L)} \end{cases} \tag{28}$$

$$\left(\frac{\Delta x}{x}\right)_{max} = \frac{x^*}{x_{max}} - 1 = \begin{cases} -1/n_\Delta & \text{if } n_{\ell x} > 0 \text{ and } n_{rx} > 0 \text{ (Zone R)} \\ -1/(2\bar{n}_x) & \text{if } n_{\ell x} > 0 \text{ and } n_{rx} < 0 \text{ (Zone M)} \\ 1/n_\Delta & \text{if } n_{\ell x} < 0 \text{ and } n_{rx} < 0 \text{ (Zone L)} \end{cases} \tag{29}$$

$$\left(\frac{\Delta y}{y}\right)_{min} = \frac{y^*}{y_{min}} - 1 = \frac{1}{n_\Delta} \tag{30}$$

$$\left(\frac{\Delta y}{y}\right)_{max} = \frac{y^*}{y_{max}} - 1 = -\frac{1}{n_\Delta} \tag{31}$$

$$\left(\frac{\Delta z}{z}\right)_{min} = \frac{z^*}{z_{min}} - 1 = \begin{cases} (2\bar{n}_z + n_\Delta - 1)/[2(\bar{n}_z - 1)n_\Delta] & \text{if } \bar{n}_z > \tfrac{1}{2} \\ (-2n_z + n_\Delta + 1)/[2(\bar{n}_z - 1)n_\Delta] & \text{if } \bar{n}_z \le \tfrac{1}{2} \end{cases} \tag{32}$$

$$\left(\frac{\Delta z}{z}\right)_{max} = \frac{z^*}{z_{max}} - 1 = \begin{cases} (-2\bar{n}_z - n_\Delta + 1)/(2\bar{n}_z n_\Delta) & \text{if } \bar{n}_z \ge \tfrac{1}{2} \\ (\bar{n}_z - n_\Delta - 1)/(\bar{n}_z n_\Delta) & \text{if } \bar{n}_z < \tfrac{1}{2} \end{cases} \tag{33}$$

7. Space of View

The effect of the size of the image plane will now be considered, assuming that the image plane is a w X w square. The widest space viewed from each camera is a pyramid formed by the straight lines connecting each lens with the corners of its square image plane. The top view along the -z direction and the side view along the -x direction of the two pyramids are shown in Fig. 9. The half-infinite space in front of the two cameras is divided into three spaces: (1) the space not seen by any camera, (2) the space seen by only one camera, and (3) the space seen by both cameras. The top and side views of the third space are shaded in Fig. 9, and each is characterized by the view angle

$$\beta = 2 \tan^{-1} \frac{w}{2f} \quad . \tag{34}$$

Clearly, only this tent-shaped space is effective for stereo applications. The distance between the origin (midpoint between the lenses) and the tip of the effective space is

$$r_m = f\frac{D}{w} \quad . \tag{35}$$

This is the minimum distance that can be determined by the stereoscopic setup.

8. Numerical Example

Let us consider a numerical example in which D = 6" = 152 mm, f = 16 mm, w = 10 mm, and the image plane is quantized into 120 X 120 cells. We wish to determine the effective stereopsis space, the analog and quantized image coordinates associated with an object point located at $v = (10^3 \text{ mm}, 10^4 \text{ mm}, 2 \cdot 10^3 \text{ mm})^t$, and the uncertainty space that corresponds to the image quantized data (if these data were given).

(1) Effective Stereopsis Space

Using (34) and (35),

$$\theta = w \tan^{-1} \frac{10}{2 \cdot 16} = 34.7^\circ$$

and

$$r_m = 16 \frac{152}{10} = 243 \text{ mm.}$$

(2) Image Coordinates

The quantization cell size is

$$d = \frac{w}{120} = \frac{10}{120} = \frac{1}{12} \text{ mm} = 0.0833 \text{ mm.}$$

Modifying (2), $x_\Delta = \frac{Df}{y} = \frac{152 \cdot 16}{10^4} = 0.243$ mm.

Modifying (1), $\bar{x}_p = \frac{x_\Delta}{D} x = \frac{0.243}{152} \cdot 10^3 = 1.6$ mm.

Modifying (8), $\bar{z}_p = \frac{x_\Delta}{D} z = \frac{0.243}{152} \cdot 2 \cdot 10^3 = 3.2$ mm.

Solving for x_ℓ and x_r, we get

$$x_\ell = \tfrac{1}{2} (2x_p + x_\Delta) = \tfrac{1}{2} (3.2 + 0.243) = 1.7215 \text{ mm}$$

$$x_r = \tfrac{1}{2} (2x_p - x_\Delta) = \tfrac{1}{2} (3.2 - 0.243) = 1.4785 \text{ mm.}$$

The image quantization numbers are

$$n_{\ell x} = \lceil x_\ell / d \rceil^* = \lceil 1.7215/0.0833 \rceil = \lceil 20.7 \rceil = 21$$

$$n_{rx} = \lceil x_r / d \rceil = \lceil 1.4785/0.0833 \rceil = \lceil 17.7 \rceil = 18$$

$$\bar{n}_z = \lceil \bar{z}_p / d \rceil = \lceil 3.2/0.0833 \rceil = \lceil 38.4 \rceil = 39$$

Following (11) through (20),

$$x_\ell^* = (n_{\ell x} - \tfrac{1}{2}) d = 20.5 \cdot 0.0833 = 1.71 \text{ mm}$$

$$x_r^* = (n_{rx} - \tfrac{1}{2}) d = 17.5 \cdot 0.0833 = 1.46 \text{ mm}$$

---

* We shall use the notation

$\lceil x \rceil \equiv$ round up integer $\geq x$

$\lfloor x \rfloor \equiv$ round down integer $\leq x$

$$n_{\Delta} = 21 - 18 = 3$$

$$\bar{n}_x = \tfrac{1}{2}(21 + 18) = 19.5$$

$$x_{\Delta}^* = 3 \cdot 0.0833 = 0.25 \text{ mm}$$

$$\bar{x}_p^* = (19.5 - 0.5) \cdot 0.0833 = 1.585 \text{ mm}$$

$$\bar{z}_p^* = (39 - 0.5) \cdot 0.0833 = 3.21 \text{ mm.}$$

Following (21),

$$v^* = \begin{pmatrix} x^* \\ y^* \\ z^* \end{pmatrix} = \begin{pmatrix} 152 \cdot 19/3 \\ 152 \cdot 16/(3 \cdot 0.0833) \\ 152 \cdot 38.5/3 \end{pmatrix} = \begin{pmatrix} 963 \\ 9{,}730 \\ 1{,}950 \end{pmatrix} \text{(mm)}$$

The absolute errors are, therefore,

$$\Delta v = \begin{pmatrix} x^* - x \\ y^* - y \\ z^* - z \end{pmatrix} = \begin{pmatrix} -37 \\ -270 \\ -50 \end{pmatrix} \text{ (mm)}$$

The corresponding relative errors are

$$\begin{pmatrix} \Delta x/x \\ \Delta y/y \\ \Delta z/z \end{pmatrix} = \begin{pmatrix} (x^*-x)/x \\ (y^*-y)/y \\ (z^*-z)/z \end{pmatrix} = \begin{pmatrix} -37/1{,}000 \\ -270/10{,}000 \\ -50/2{,}000 \end{pmatrix} = \begin{pmatrix} -0.037 \\ -0.027 \\ -0.025 \end{pmatrix}$$

(3) Uncertainty Space

Following (22) through (27),

$$x_{min} = 152 \cdot 19/4 = 722.5 \text{ mm}$$

$$x_{max} = 152 \cdot 19/2 = 1{,}445 \text{ mm}$$

$$y_{min} = \frac{152 \cdot 16}{0.0833 \cdot 4} = 7{,}300 \text{ mm}$$

$$y_{max} = \frac{152 \cdot 16}{0.0833 \cdot 2} = 14{,}600 \text{ mm}$$

$$z_{min} = 152 \cdot 38/4 = 1{,}445 \text{ mm}$$

$$z_{max} = 152 \cdot 39/2 = 2{,}962 \text{ mm.}$$

Thus, the best estimate and the uncertainty space of $v = (x, y, z)^t$ are

$$x^* = 963 \text{ mm}; \quad 722.5 < x < 1{,}445 \text{ mm}$$

$$y^* = 9{,}730 \text{ mm}; \quad 7{,}300 < y < 14{,}600 \text{ mm}$$

$$z^* = 1{,}950 \text{ mm}; \quad 1{,}445 < z < 2{,}962 \text{ mm}.$$

The resulting relative uncertainty space is defined by $-0.33 < \Delta x/x < 0.33$, $-0.33 < \Delta y/y < 0.33$, and $-0.34 < \Delta z/z < 0.35$. These results agree with (28) through (33) in which $n_\Delta = 3$ and $\bar{n}_z = 39$.

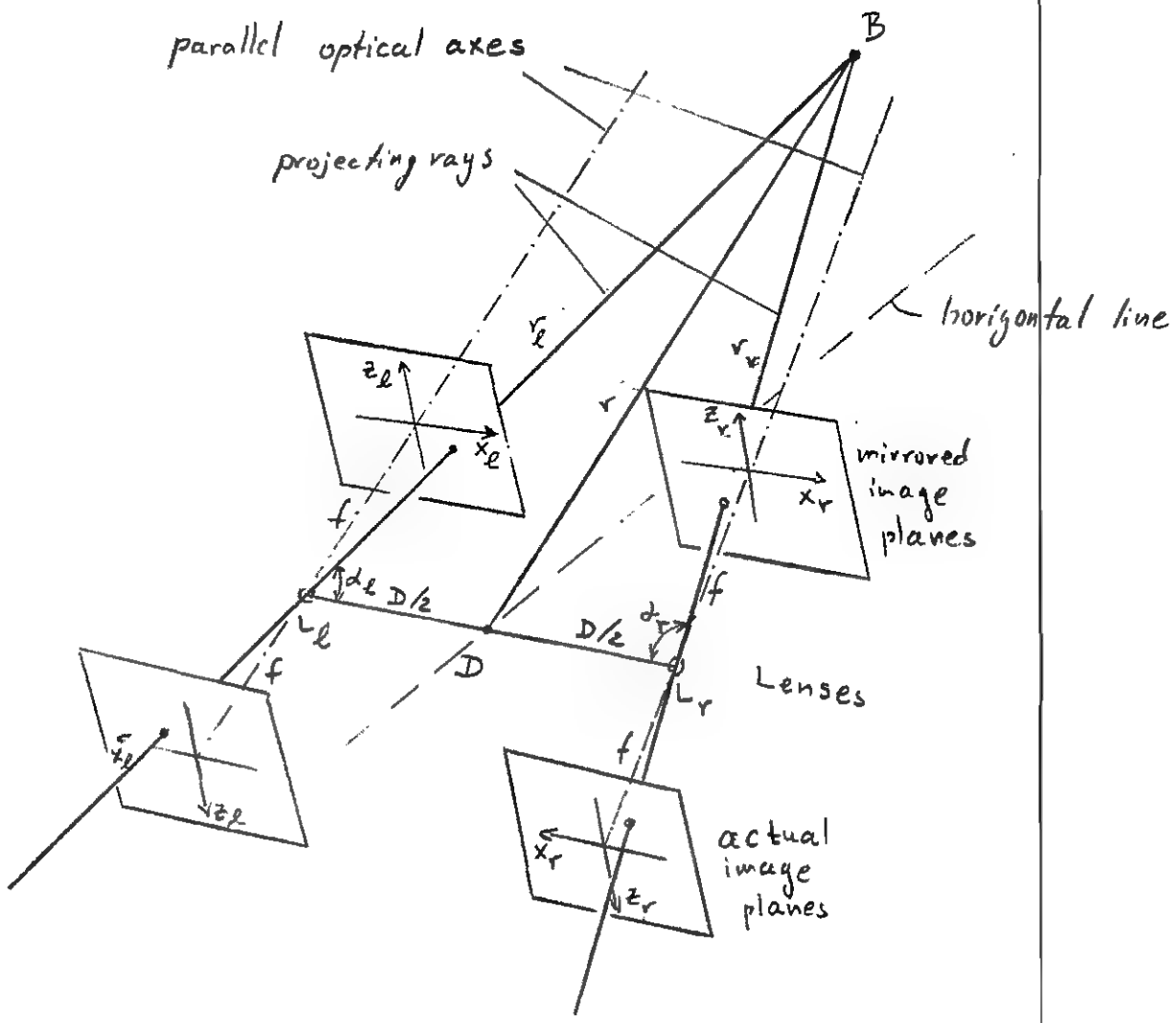

Fig. 1 Geometry of steriuscopic pictures

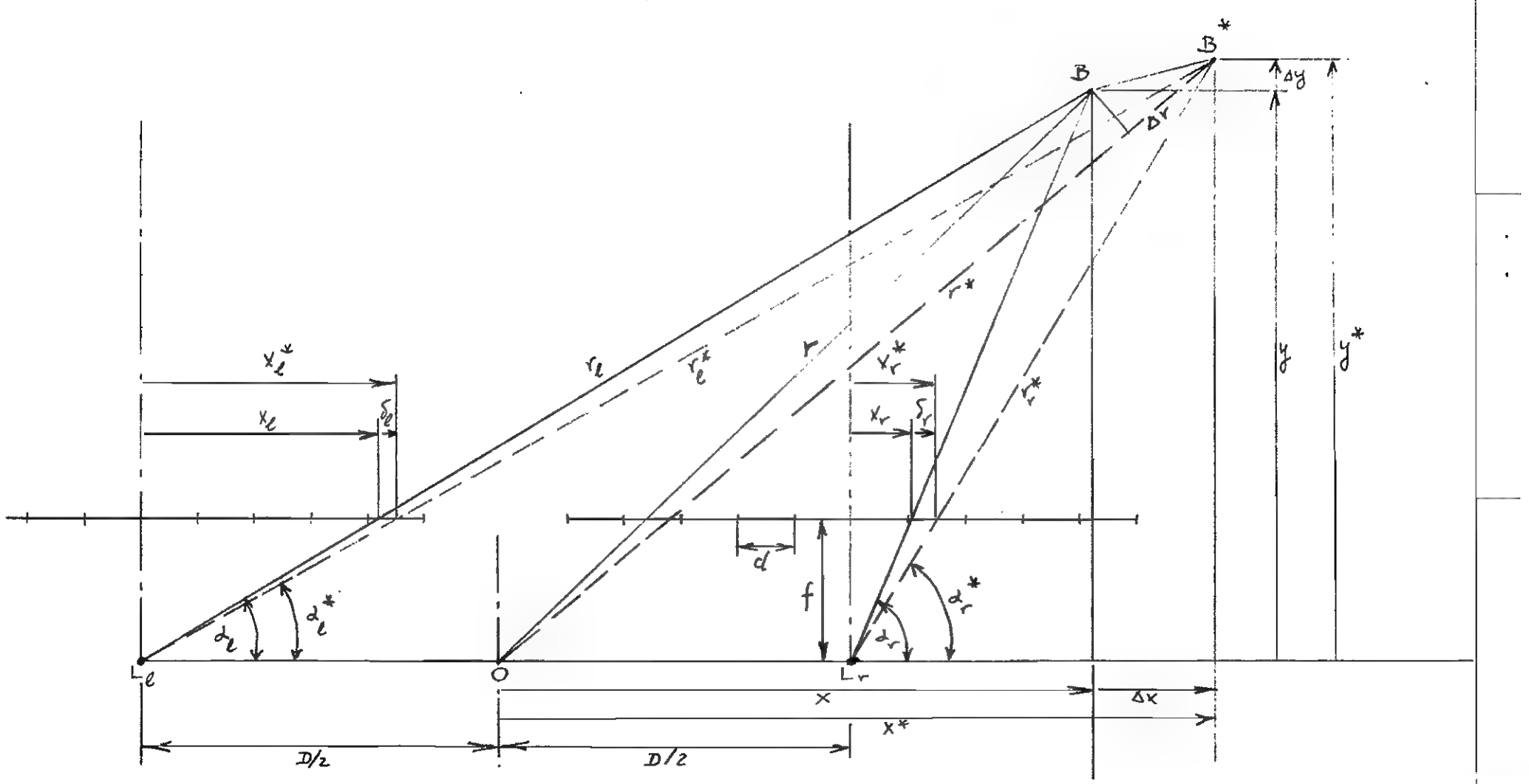

Fig. 2 Top view of stereopsis plane

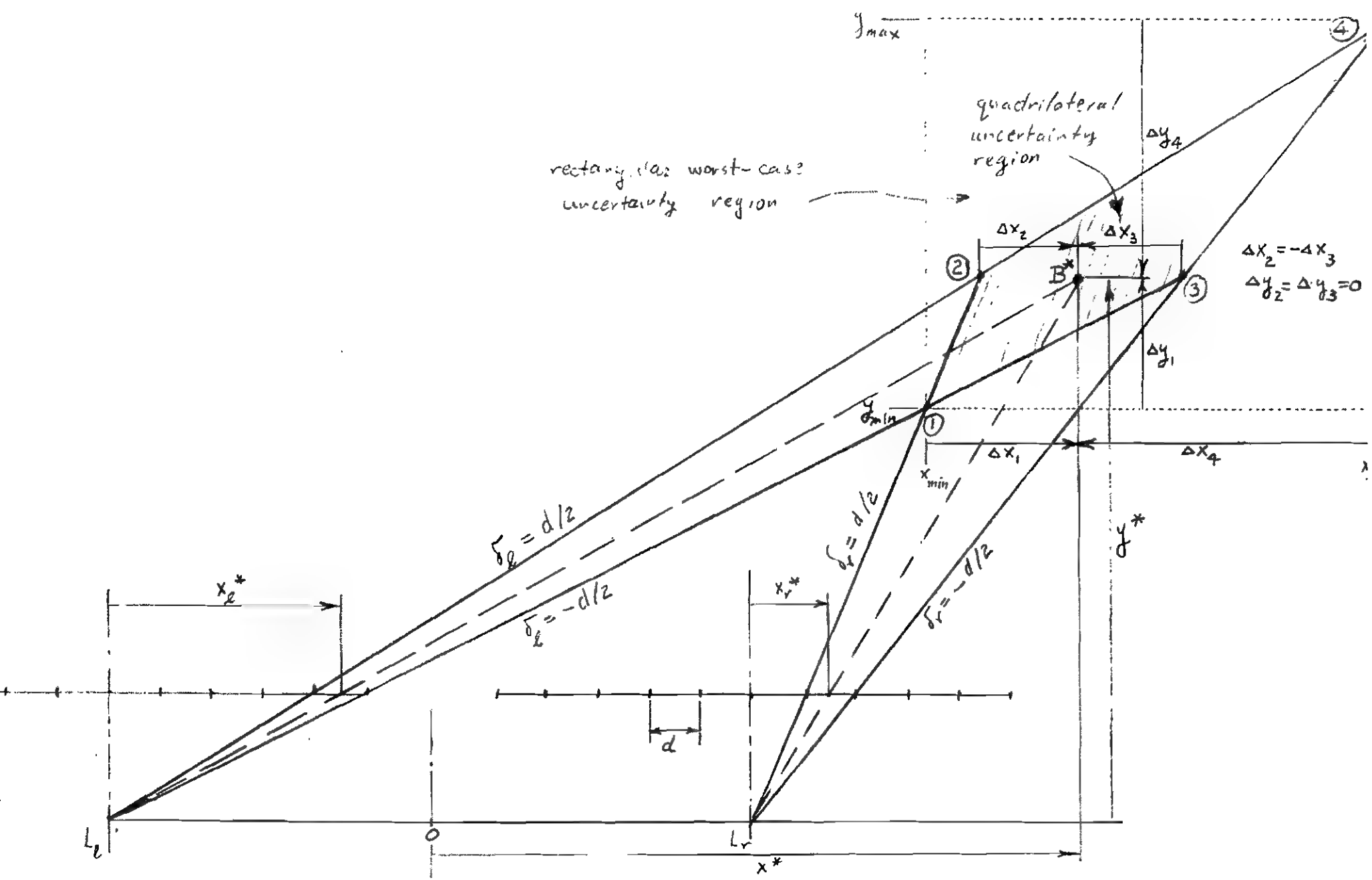

Fig. 3 Quadrilateral and rectangular (worst-case) uncertainty regions

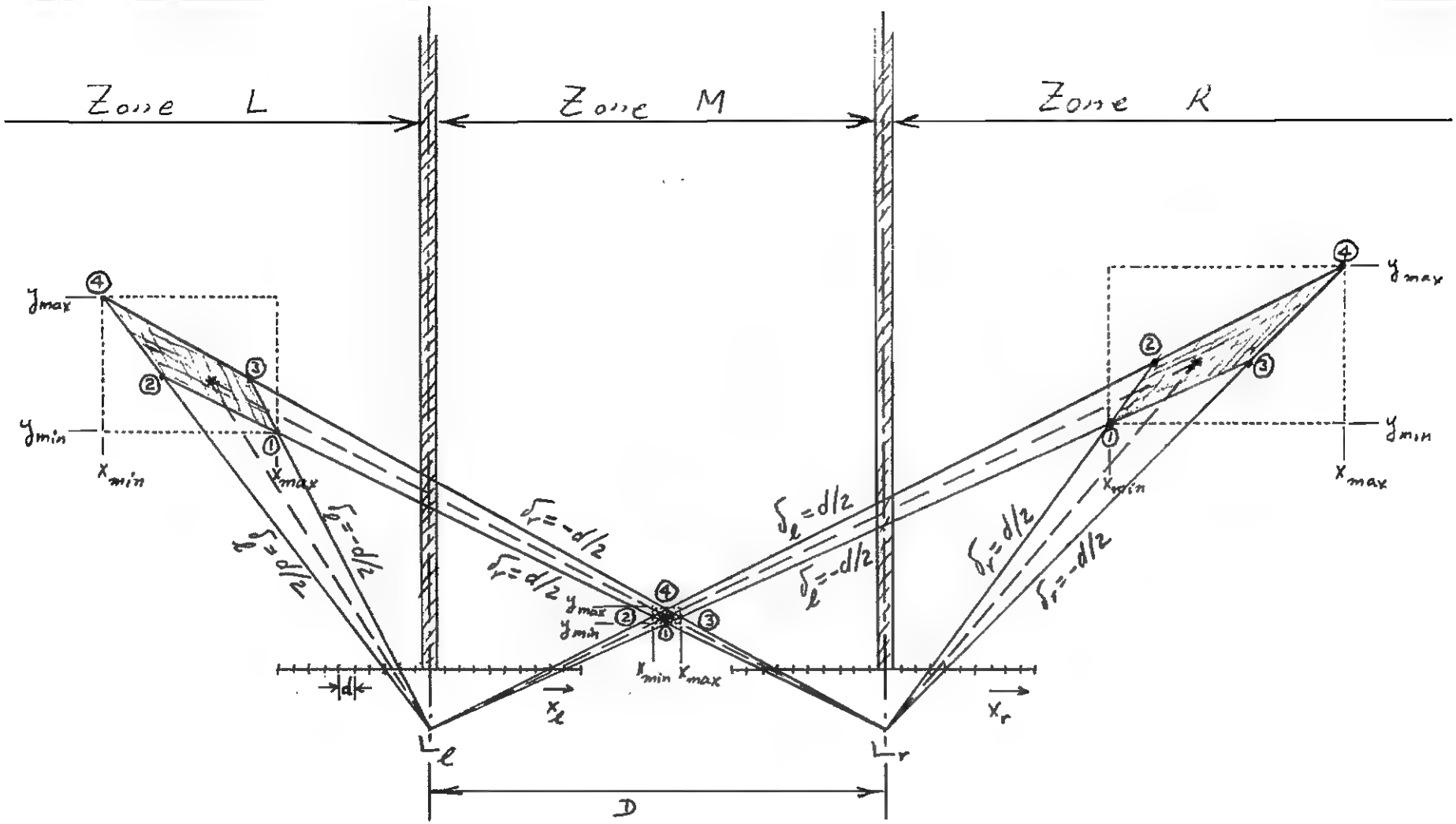

Fig. 4 Uncertainty regions in the three possible zones

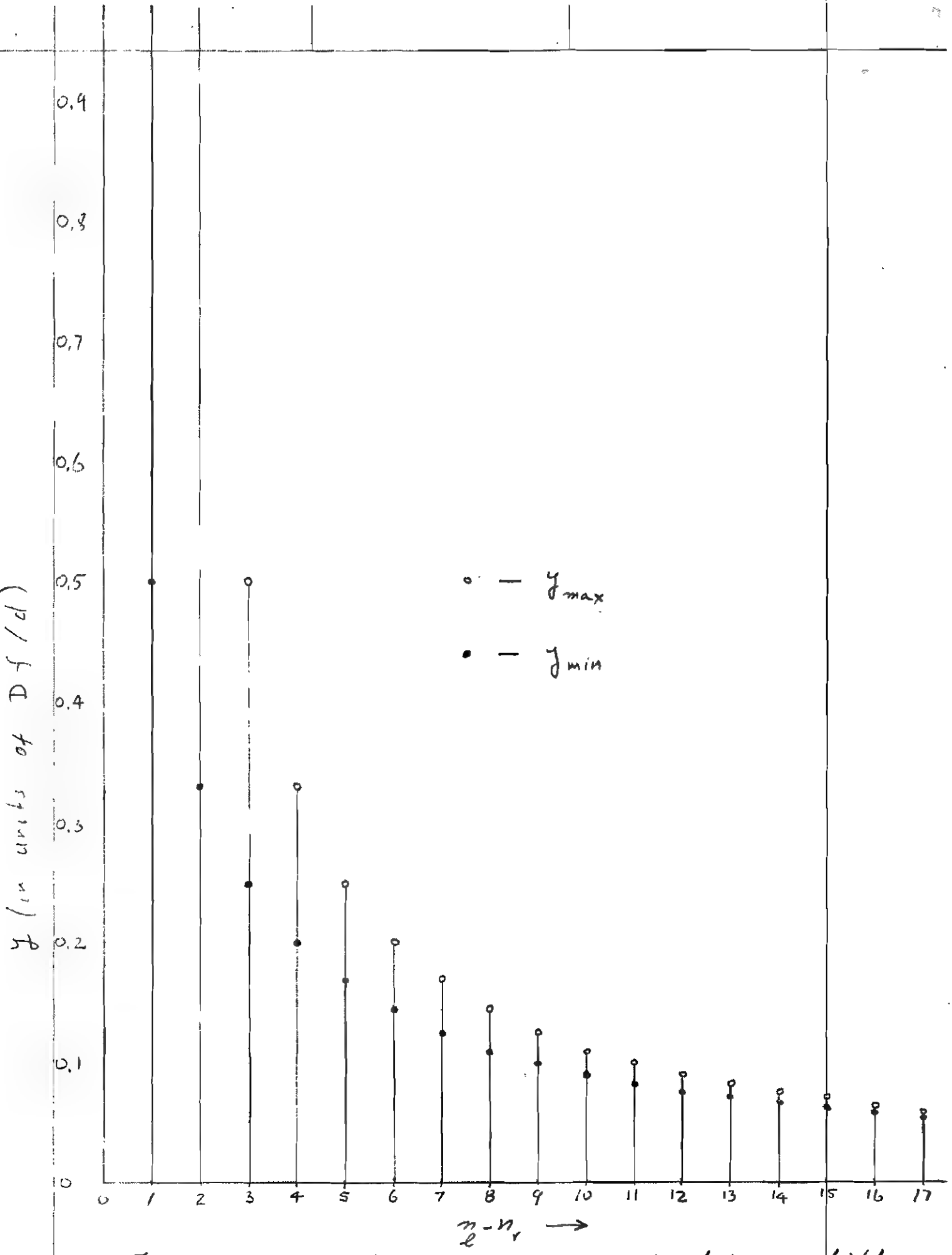

Fig. 5 γ_{min} and γ_{max} vs. quantized image shift

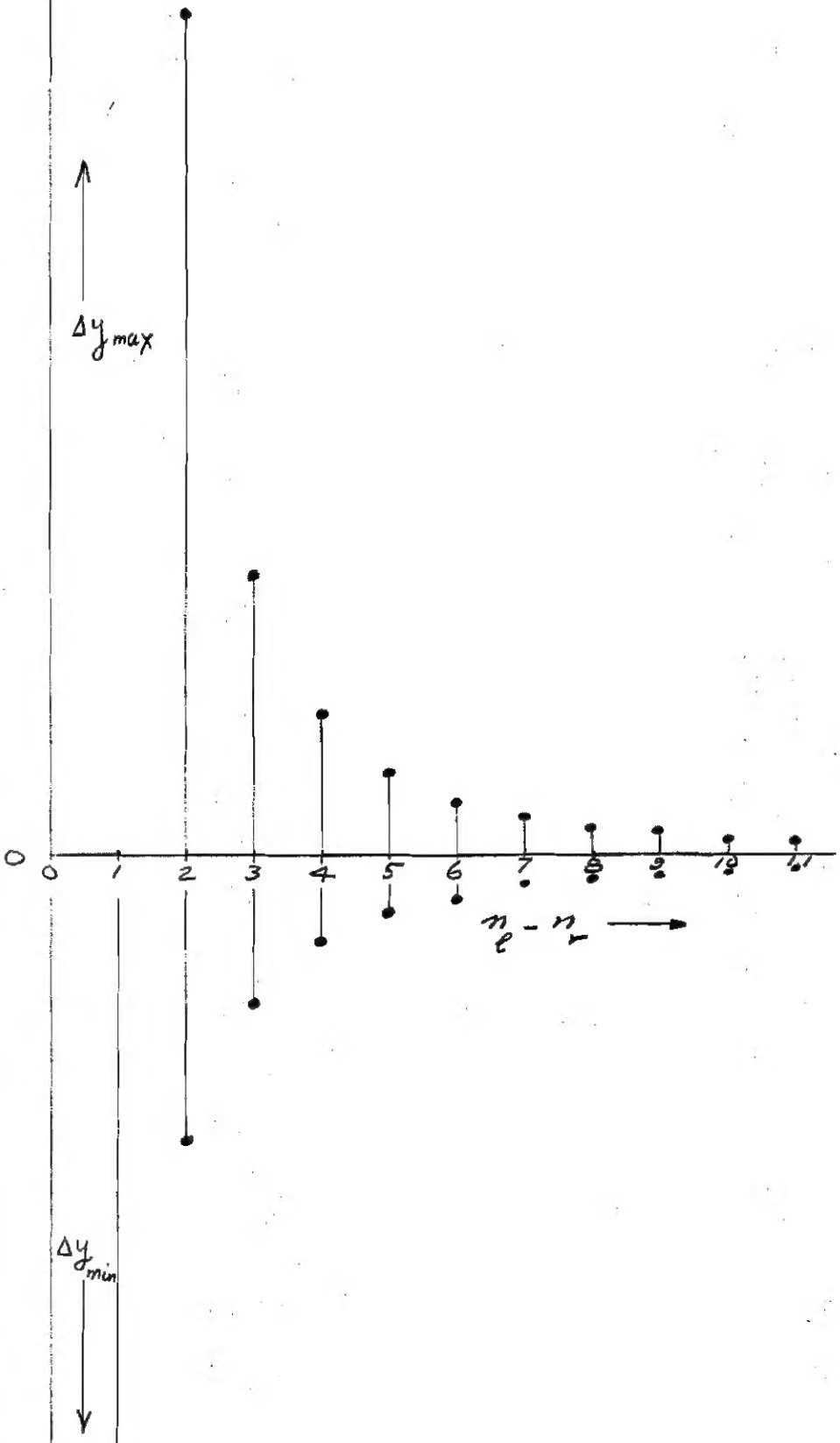

Fig. 6 Δy_{min} and Δy_{max} vs. quantized image shift

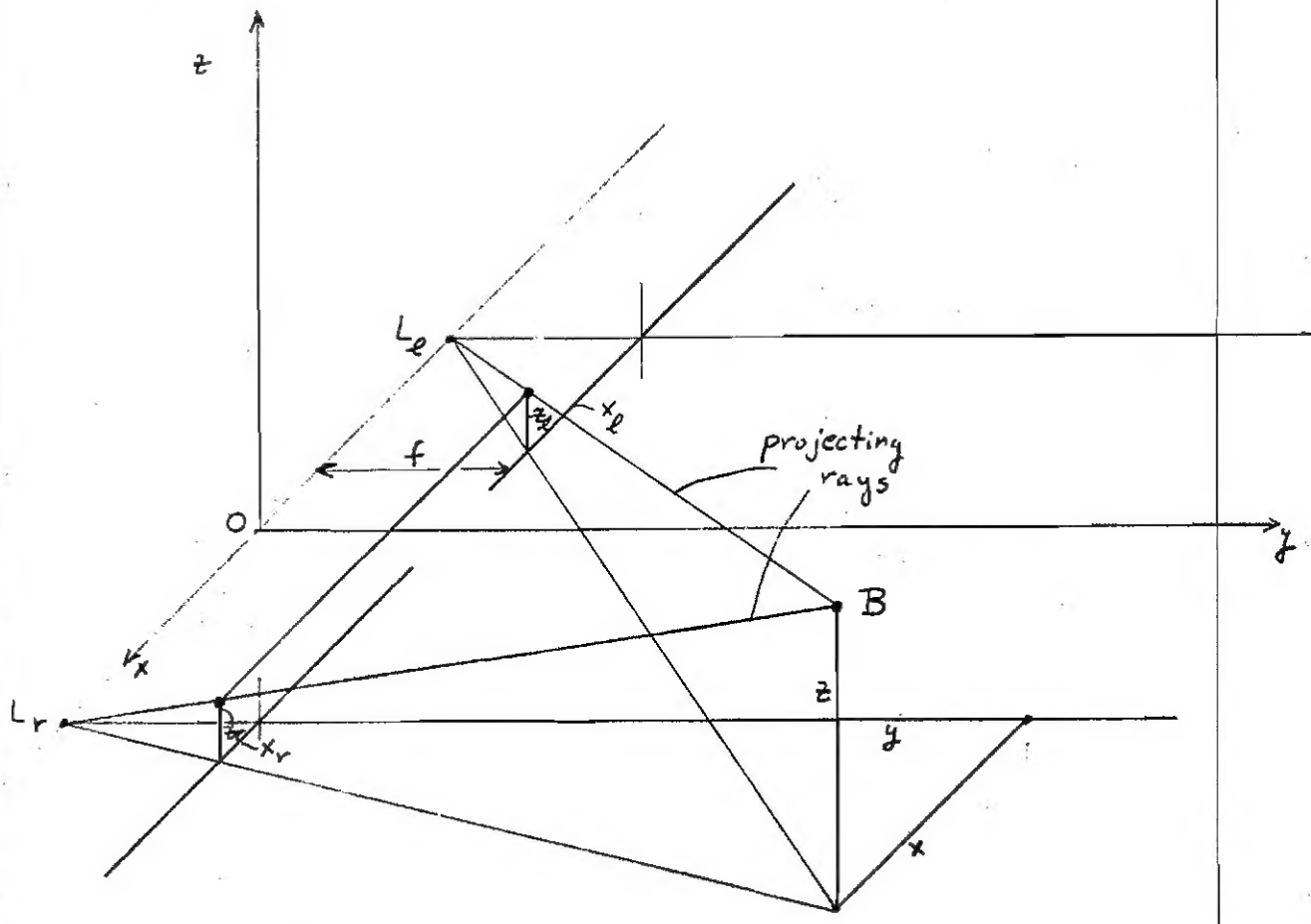

Fig. 7 Stereopsis of a point in 3-d space

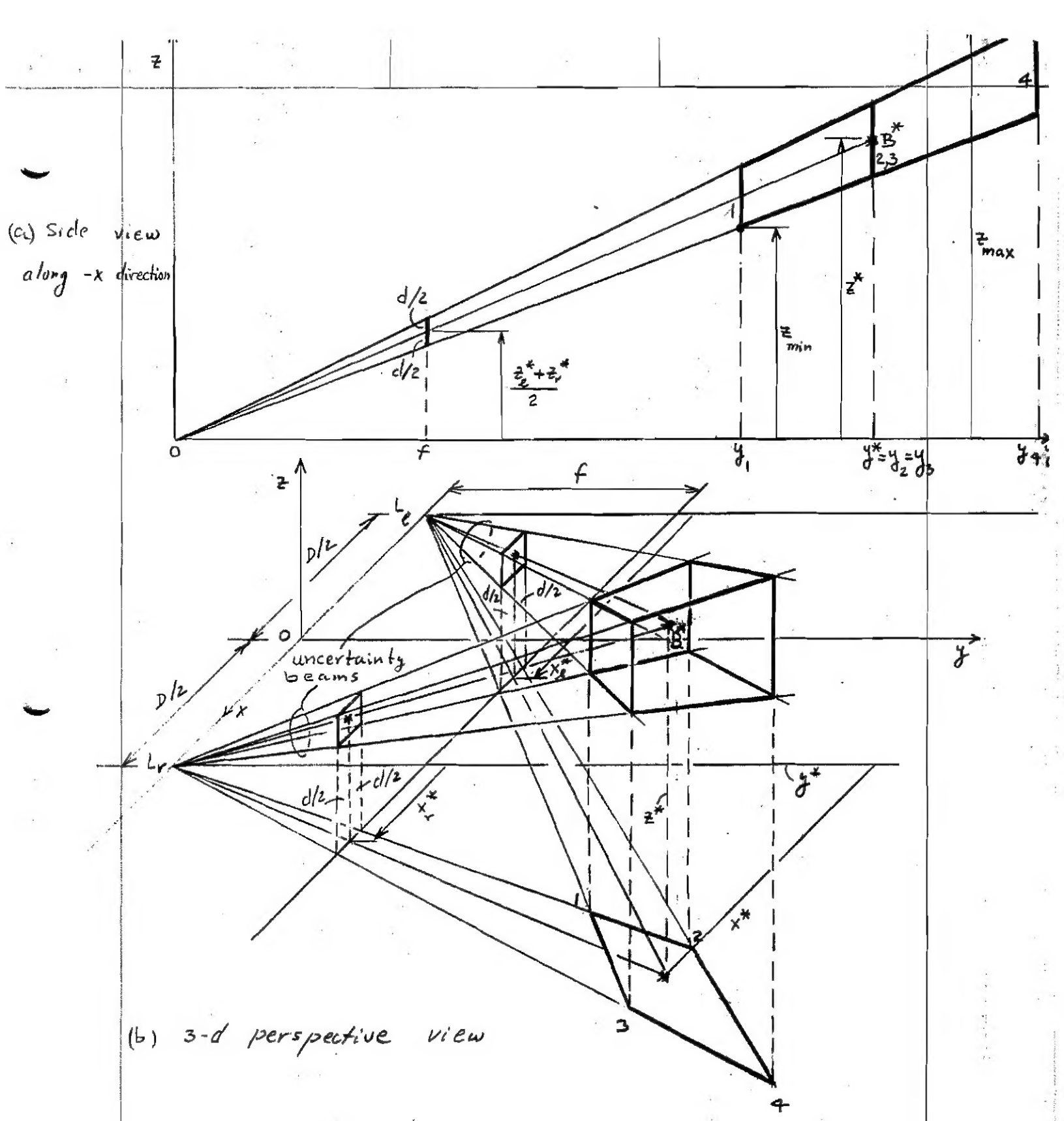

Fig. 8 Hexahedral uncertainty space

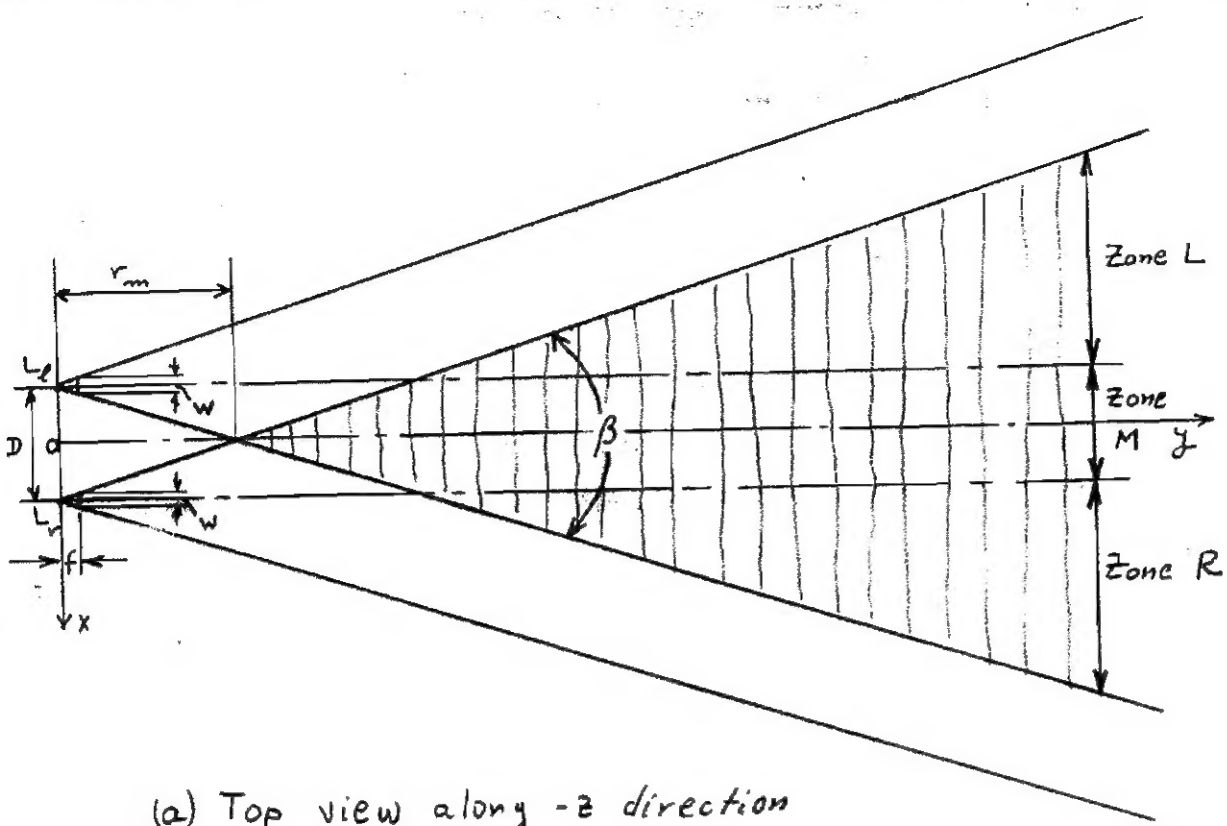

(a) Top view along -z direction

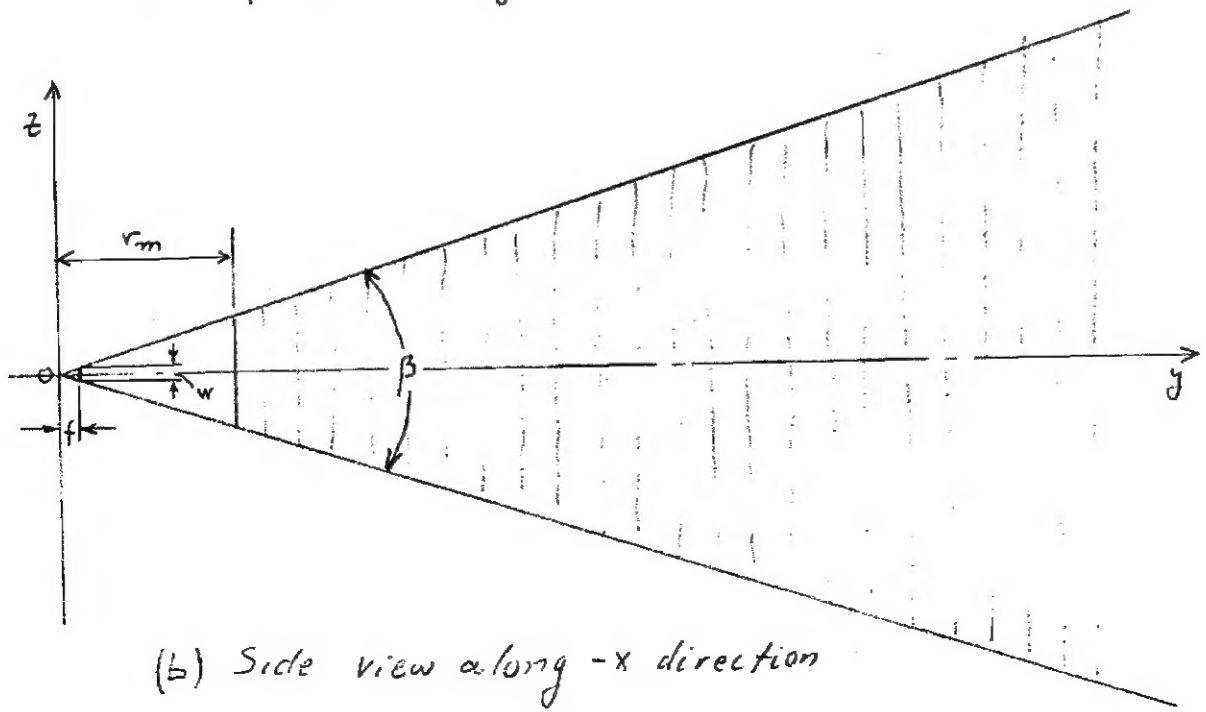

(b) Side view along -x direction

Fig. 9 Effective tent-shaped stereopsis space